AIP | Applied Physics Letters

Uniaxial anisotropy of two-magnon scattering in an ultrathin epitaxial Fe layer on GaAs

H. Kurebayashi, T. D. Skinner, K. Khazen, K. Olejník, D. Fang et al.

Citation: Appl. Phys. Lett. **102**, 062415 (2013); doi: 10.1063/1.4792269
View online: http://dx.doi.org/10.1063/1.4792269
View Table of Contents: http://apl.aip.org/resource/1/APPLAB/v102/i6
Published by the American Institute of Physics.

Related Articles

First principles study of magnetic anisotropy and magnetoelectric effect of FePd/MgO(001) ultrathin films
J. Appl. Phys. 113, 17C702 (2013)

Electric-voltage control of magnetism in Fe/BaTiO3 heterostructured multiferroics
J. Appl. Phys. 113, 17C701 (2013)

Reducing the writing field of L10-FePt by graded order parameter
J. Appl. Phys. 113, 073912 (2013)

Nonlinear susceptibility and dynamic hysteresis loops of magnetic nanoparticles with biaxial anisotropy
J. Appl. Phys. 113, 053903 (2013)

The over-barrier reflection of the Bloch point in uniaxial ferromagnets with strong magnetic anisotropy
Low Temp. Phys. 39, 151 (2013)

Additional information on Appl. Phys. Lett.

Journal Homepage: http://apl.aip.org/
Journal Information: http://apl.aip.org/about/about_the_journal
Top downloads: http://apl.aip.org/features/most_downloaded
Information for Authors: http://apl.aip.org/authors

ADVERTISEMENT

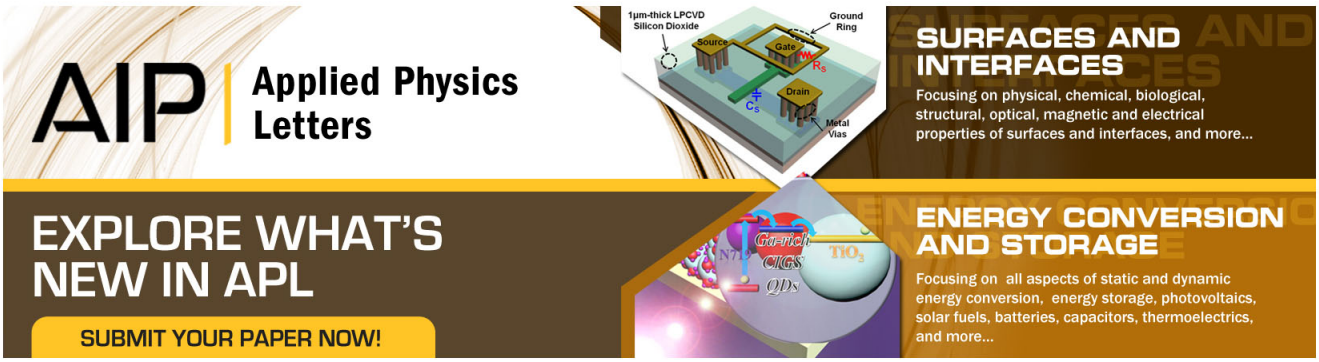

Uniaxial anisotropy of two-magnon scattering in an ultrathin epitaxial Fe layer on GaAs

H. Kurebayashi,[1,2,a)] T. D. Skinner,[1] K. Khazen,[3,b)] K. Olejník,[4,c)] D. Fang,[1] C. Ciccarelli,[1] R. P. Campion,[3] B. L. Gallagher,[3] L. Fleet,[5] A. Hirohata,[2,5] and A. J. Ferguson[1]
[1]*Cavendish Laboratory, University of Cambridge, J. J. Thomson Avenue, Cambridge CB3 0HE, United Kingdom*
[2]*PRESTO, Japan Science and Technology Agency, Kawaguchi 332-0012, Japan*
[3]*School of Physics and Astronomy, University of Nottingham, Nottingham NG7 2RD, United Kingdom*
[4]*Hitachi Cambridge Laboratory, J. J. Thomson Avenue, Cambridge CB3 0HE, United Kingdom*
[5]*Department of Electronics, University of York, Heslington, York YO10 5DD, United Kingdom*

(Received 3 September 2012; accepted 29 January 2013; published online 13 February 2013)

We report an on-chip, electrically detected ferromagnetic resonance study on microbars made from GaAs/Fe(1 nm)/GaAs layers. Our experiments, performed at several different microwave frequencies and static magnetic field directions, enable us to observe a strong in-plane uniaxial anisotropy of the linewidth. We attribute the linewidth anisotropy to the two magnon scattering process, supporting this by calculations of possible linewidth broadening mechanisms. Our findings are useful for designing future high-performance spintronic devices based on nanoscale magnetic structures. © *2013 American Institute of Physics*. [http://dx.doi.org/10.1063/1.4792269]

Magnetic relaxation processes govern the efficiency and power consumption of spintronic devices.[1] Successful switching of the magnetic state generally occurs when the rate of non-equilibrium torque produced in each magnetic cell for memory or logic application (e.g., spin transfer torque[2]) overcomes the rate of magnetic relaxation.[3] In a rapidly growing field called magnonics,[4,5] where propagating spin-waves can be an information carrier to develop spin-based electric devices, magnetic relaxation parameters determine the propagation efficiency (or decay rate) of these spin-waves. When it comes to generation of pure spin currents (a flow of angular momentum without charge current) by magnetic dynamics (spin pumping[6–9]), the amount of spin current is known to be inversely proportional to the square of the damping coefficient.[10] Hence, a better understanding of magnetic relaxation physics aids development of future low-power consumption and functional spintronic devices.

Magnetic relaxation processes are paths of energy and angular momentum dissipation from the excited spin-wave states directly to the lattice or to other spin-wave states.[11] The former gives the Gilbert damping term in the Landau-Lifshitz-Gilbert equation.[12] The spin-spin coupling causes the other dissipative processes, including multi-magnon interactions. We note that recently the three-magnon splitting, one of the multi-magnon interactions, shows potential for generating spin currents.[13] In addition to the three-magnon process, there is a commonly known two-magnon process,[14] where one spin-wave mode scatters into a different mode with changing its wavevector k. Defects in a crystal are key to induce the two-magnon processes since around the defects the translational symmetry in space is broken, which allows scattering processes where k is not conserved. These two magnon processes become more important in nano-scale ferromagnets[15,16] since defects are more often present and effective due to the lager volume ratio of surface/interface in the nanostructures. In this paper, we report on two-magnon scattering in an ultra-thin epitaxial Fe layer on GaAs. We employed electrical on-chip ferromagnetic resonance (FMR) techniques to measure Fe micro-bars and extract material parameters of magnetic anisotropies and dynamics in the Fe film. There are a good number of experimental reports on two-magnon scattering in thin-film ferromagnets.[17–26] We here show a strong uniaxial anisotropy of the two-magnon scattering in the Fe/GaAs system. Tuning the two-magnon scattering efficiency by changing the in-plane magnetic field direction, we observed the linewidth change by a factor of four between the easy and hard axes.

GaAs and epitaxial Fe layers were grown in a single MBE chamber without breaking vacuum between the layer growths. The layer structure is GaAs-cap (20 nm)/Fe (1.0 nm)/GaAs-buffer (500 nm)/GaAs substrate. All the layers are non-doped, epitaxially grown except for the top polycrystalline GaAs layer. A $4 \times 20\ \mu$m micro-bar (the SEM image shown in Fig. 1(a)) was defined on the sample using standard photolithography and ion-milling techniques. The device was mounted on a microwave board in order to carry out on-chip electrical FMR measurements at room temperature. A microwave current injected into the sample exerted FMR that produced a dc voltage across the sample (schematic shown in Fig. 1(a)). This is because mixing of a microwave current and the resistance change arising from anisotropic magnetoresistance and magnetization precession produces the dc voltage.[27–30] The microwave current was pulse-modulated at 23 Hz and the voltage at the modulation frequency was measured by lock-in detection techniques; we call this "V_{dc}" in this paper. Figure 1(b) shows typical FMR scans in our sample which have the following two components as

[a)]Email: hk295@cam.ac.uk.
[b)]Present address: Université Pierre et Marie Curie Institut des NanoSciences de Paris 4 place Jussieu, 75252 Paris, France.
[c)]Present address: Institute of Physics ASCR, v.v.i., Cukrovarnická 10, 162 53 Praha 6, Czech Republic.

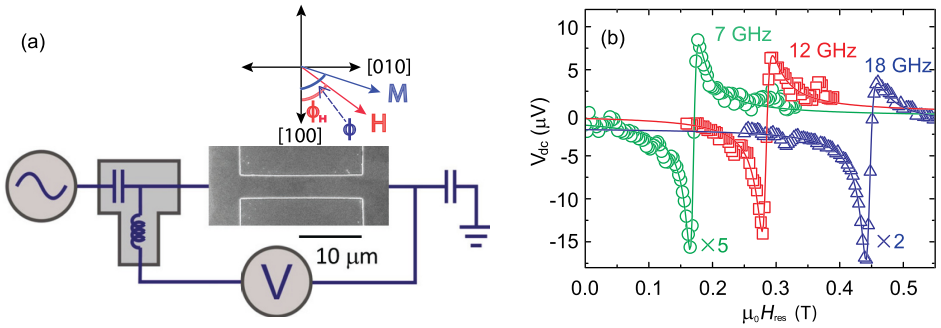

FIG. 1. (a) SEM image of the Fe microbar with the schematic of measurement circuit used for this study and the definition of orientations used in this paper. (b) Typical FMR traces on detected dc voltages across the Fe bar for different frequencies ($\phi_H = 45°$). Measured voltages are represented by dots and the fit curves are produced by Eq. (1).

$$V_{dc} = V_{sym}\frac{\Delta H^2}{(H-H_{res})^2+\Delta H^2} + V_{asy}\frac{\Delta H(H-\Delta H)}{(H-H_{res})^2+\Delta H^2}, \quad (1)$$

where H, H_{res}, ΔH, V_{sym}, and V_{asy} are the applied dc magnetic field, the resonance field and the linewidth of the FMR resonance, prefactors of the symmetric and antisymmetric terms (see the detailed expressions in Ref. 30). Using this equation and various FMR measurements, we extracted all the key parameters of magnetic anisotropy and relaxation in our ultra-thin Fe film.

We first show H_{res} measured as a function of in-plane angle ϕ_H and frequency f in Fig. 2. In-plane FMR conditions for a cubic ferromagnetic thin-film can be obtained using its free energy expression and the modified Kittel formula as[31]

$$\begin{aligned}(\omega/\gamma)^2 = {} & \mu_0^2\{M_{eff} + H_2\sin^2(\phi-\phi_0) + H\cos(\phi-\phi_H)\} \\ & \times\{H_4\cos(4\phi) - H_2\cos 2(\phi-\phi_0) \\ & + H\cos(\phi-\phi_H)\}. \end{aligned} \quad (2)$$

Here, ω, γ, M_{eff}, H_2, H_4, ϕ_H, and ϕ are angular frequency, the gyromagnetic ratio, effective magnetization, in-plane uniaxial and cubic anisotropy fields, angles of the magnetic field and magnetization with respect to the [100] crystallographic direction. ϕ_0 is the hard-axis direction of the in-plane uniaxial anisotropy. Using this equation to fit H_{res} in Figs. 2(a) and 2(b) simultaneously, we found the best parameters as $\mu_0 H_2 = 0.108\,\mathrm{T}$, $\mu_0 M_{eff} = 0.645\,\mathrm{T}$, $\gamma = 187\,\mathrm{rad\ GHz/T}$ with negligible H_4 term contribution. This dominant H_2 behavior along $(1\bar{1}0)$ direction is consistent with previous reports for ultra-thin Fe on GaAs.[32]

We now turn to the magnetic relaxation analysis of our study. There are intrinsic and extrinsic contributions to the FMR linewidth ΔH. The in-plane and frequency dependence of ΔH can be expressed as

$$\begin{aligned}\Delta H = {} & \Delta H_{inhom} + \frac{2\pi\alpha f}{\mu_0\gamma\Phi} + \left|\frac{\partial H_{res}}{\partial\phi_H}\Delta\phi_H\right| \\ & + \sum_i \frac{\Gamma_i^0 f_i(\phi_H)}{\mu_0\gamma\Phi}\sin^{-1}\sqrt{\frac{\sqrt{\omega^2+(\omega_0/2)^2}-\omega_0/2}{\sqrt{\omega^2+(\omega_0/2)^2}+\omega_0/2}}, \end{aligned} \quad (3)$$

$$\Phi = (d\omega^2/dH)/(\mu_0^2\gamma^2(W_x+W_y)).$$

The first term is due to the inhomogeneity of the sample and is independent of both frequency and in-plane angle. The second is the phenomenological Gilbert damping term with α as the dimensionless coefficient, which is intrinsic in magnetic materials and dependent on the frequency.[12] When $\phi_H \neq \phi$, a correction factor Φ due to the field dragging effect plays a role in linewidth broadening;[26,33] here, W_x and W_y are the stiffness fields, i.e., for the FMR frequency $\omega_{FMR} = \gamma^2 W_x W_y$. A spatial variation of magnetic anisotropies over a sample causes a linewidth broadening represented by the third mosaicity term.[19] The last term is the contribution of two-magnon scattering.[16] This magnon process occurs when an excited spin-wave has degenerate states to relax down to by defects. In typical ferromagnetic materials, a uniform FMR state ($k = 0$) has degenerate high k spin-wave states (although this depends on the applied magnetic field). Hence, when a FMR mode is excited during normal FMR measurements, the two-magnon scattering leads this mode to the degenerate $k \neq 0$ mode as depicted in Fig. 3(a). The two-magnon scattering process has in-plane angle dependence that is represented by $\Gamma_i^0 f_i(\phi_H)$ which is the parameter of the two-magnon scattering strength.[16] In addition, $\omega_0 = \gamma\,\mu_0 M_{eff}$ and therefore the arcsine term is constant for measurements with the same frequency, like those shown in

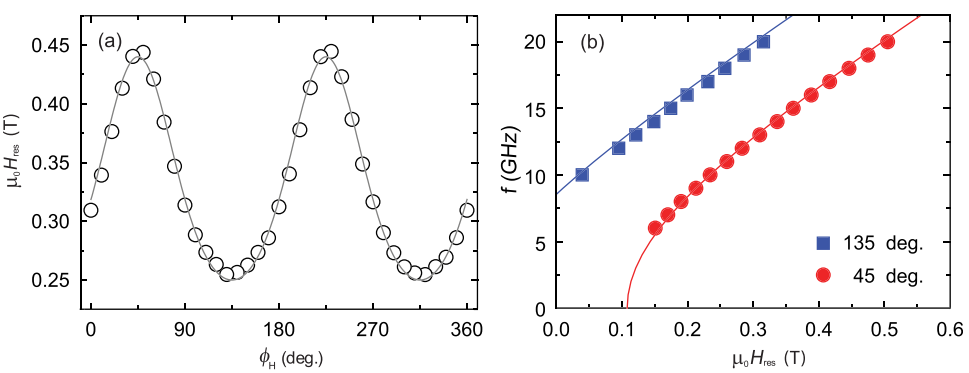

FIG. 2. Resonance field H_{res} as a function of (a) in-plane magnetic field direction ϕ_H measured at 18 GHz and (b) frequency f with fitting curves using Eq. (2). The dots and lines are measured values and fit curves, respectively.

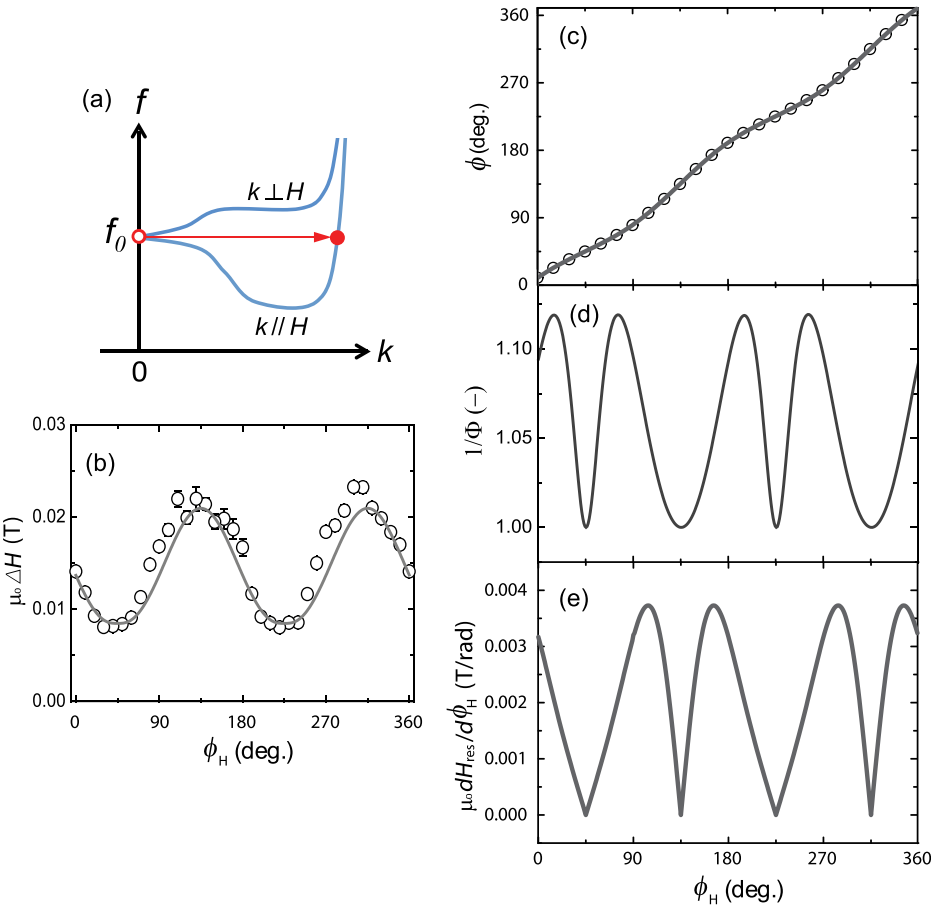

FIG. 3. (a) Schematic of a two-magnon process in spin-wave dispersion curves. The initial magnon with a state of f_0 and $k=0$ scatters into a different momentum state. (b) FMR linewidth ΔH as a function of in-plane magnetic field direction ϕ_H represented by dots, along with a curve produced by the model. The excitation field is at 18 GHz. (c) Equilibrium magnetic moment direction ϕ for measured ϕ_H (represented as dots) and a fit curve. (d) $1/\Phi$ and (e) $dH_{res}/d\phi_H$ calculated from ϕ and other FMR fit parameters.

Fig. 3(b). As can be seen in the figure, there is a strong oscillation in ΔH for different ϕ_H and the symmetry of that is two-fold. Within the expression of Eq. (3), the field dragging, mosaicity, and two-magnon scattering contributions can vary with ϕ_H. We numerically calculated ϕ using the energy-density and the modified Kittel equations and show the results in Fig. 3(c). Based on these values, we calculated the line-shape of the field dragging versus ϕ_H, shown in Fig. 3(d) and found a distorted four-fold symmetry that does not fit with ΔH measured in our device. Likewise, the calculated line-shape of the mosaicity contribution shown in Fig. 3(e) has another distorted four-fold symmetry, different from the two-fold symmetry measured. Therefore, the only remaining possibility to explain the in-plane ΔH oscillation is the two-magnon scattering with the uniaxial anisotropy in $f(\phi_H)$.

Further investigation on the presence of two-magnon scattering is possible by examining the out-of-plane scan and frequency dependence of ΔH.[16,20,22,24,34] For out-of-plane measurements starting at the in-plane magnetic easy or hard axis, the linewidth expression is given by

$$\Delta H = \Delta H_{\text{inhom}} + \frac{2\pi\alpha f}{\mu_0\gamma\Phi} + \left|\frac{\partial H_{\text{res}}}{\partial\theta_H}\Delta\theta_H\right| + \sum_i \frac{\Gamma_i^{out} f_i(\phi_H)}{\mu_0\gamma\Phi}\sin^{-1}\sqrt{\frac{\sqrt{\omega^2+(\omega_0/2)^2}-\omega_0/2}{\sqrt{\omega^2+(\omega_0/2)^2}+\omega_0/2}},$$
$$\Gamma_i^{out} = \Gamma_i^0\Phi A(\theta-\pi/4)\frac{dH_{\text{res}}(\theta_H)}{d\omega(\theta_H)}\Big/\frac{dH_{\text{res}}(\theta_H=0)}{d\omega(\theta_H=0)}. \quad (4)$$

The equation is similar to the one for in-plane, but the two-magnon strength term Γ_i^{out} is not a constant anymore but θ_H dependent. The exact expression of Γ_i^{out} is difficult to obtain since it is a function of the type and size of defects causing the two-magnon scattering[22,34] which we are unable to identify. We, therefore, take a simplified expression for Γ_i^{out} as follows. Γ_i^0 is a constant, as in for the in-plane case. $A(\theta-\pi/4)$ is a step function to express that the two-magnon scattering deactivates for $\theta<45°$ (the definition of θ is in Fig. 4(a)). This distinct cut-off feature for $\theta<45°$ arises as there are no degenerate states available for this angular region[16] and several experimental reports consistent with this exist.[20,22,24,25] The remaining part in Γ_i^{out} is a normalization factor used for the following reason. Woltersdorf and Heinrich[20] have experimentally shown that the adjusted frequency linewidth[20,35] for two-magnon scattering in their Fe/GaAs system is almost constant for $\theta>45°$ and significantly drops around $\theta=45°$ due to the term $A(\theta-\pi/4)$. By assuming that this case is applicable to our Fe/GaAs system, we set the adjusted linewidth of two-magnon scattering to be constant for $\theta>45°$ in our sample. Then, using $dH_{\text{res}}(\theta_H)/d\omega(\theta_H)$, we predict the simplified Γ_i^{out} expression as a function of θ_H. Figures 4(a)–4(c) show the out-of-plane measurements of H_{res} and ΔH, and the frequency dependence of ΔH for the two in-plane directions. The experimentally measured H_{res} is nicely fit by a curve produced with the magnetic parameters previously obtained in the in-plane measurements, from which we are able to calculate $\theta(\theta_H)$ shown in Fig. 4(b) inset. With these reliable parameters and Eq. (4), we have carried out simultaneous fits for ΔH data in

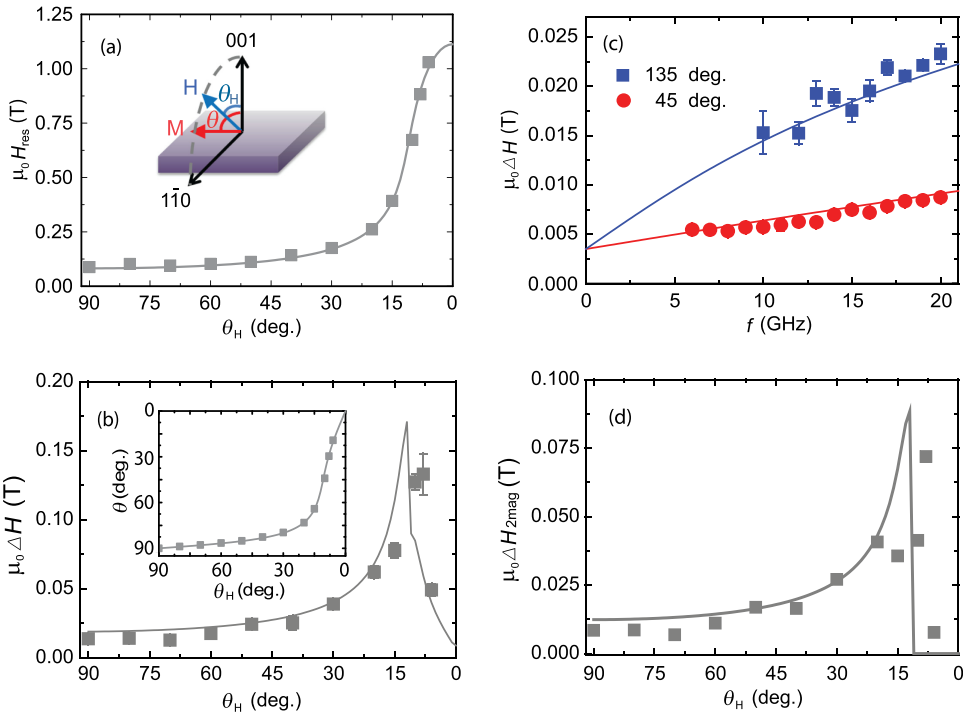

FIG. 4. (a) The resonance field H_{res}, (b) ΔH, and inset(b) the equilibrium angle θ as a function of out-of-plane angle θ_H. The dots are the experimental data measured at 12 GHz. θ is calculated from the experimental data and magnetic anisotropies. All the curves shown are the results of numerical fits. (c) Frequency dependence of ΔH for easy and hard axes represented by dots. The curves are produced by the model and best fit parameters. (d) Two-magnon linewidth component (dots) extracted by differentiating measured ΔH by the linewidth from the other components in the model. The curve is calculated by the last term in Eq. (4).

Figs. 4(b) and 4(c), which yielded fit parameters summarized in Table I where $\Gamma_{\bar{1}10} f_u(\phi_H)$ represents the two-magnon scattering strength for ϕ_H. We then proceeded to extract the linewidth originating from the two-magnon scattering by the experimental data and the fitting results, namely, using: $\Delta H_{2mag} = \Delta H - \Delta H_{inhom} - \frac{2\pi\alpha f}{\mu_0 \gamma \Phi} - \left|\frac{\partial H_{res}}{\partial \theta_H}\right| \Delta\theta_H$. ΔH_{2mag} is plotted in Fig. 4(d) for each measured θ_H point, together with the curve calculated using the last term in Eq. (4). All the ΔH data shown in Figs. 4(b)–4(d) are well-matched to the model curves, which indicate the presence of the two-magnon scattering in our sample. Furthermore, the curve in Fig. 3(b) which fits well to the data is calculated with parameters obtained by these out-of-plane fits with the uniaxial two-magnon symmetry ($\sum_i \Gamma_i f_i(\phi_H) = 0.2 + 4.5 \sin^2(\phi_H + \pi/4)$ GHz), assuming $\Delta\phi_H$ is negligible. The above analysis was also performed for another device made from the GaAs/Fe(1 nm)/GaAs wafer, and the fits provided similar parameter values summarized in Table I.

Arias and Mills have formulated the two-magnon scattering phenomena in the ultra-thin film limit.[16] The presence of two-magnon scattering on Fe/GaAs systems with the Fe thickness of 4.2(30ML) and 2.2(16ML) nm has been reported by Woltersdorf and Heinrich.[20] They have identified that misfit dislocation networks in the Fe layer acting as lattice defects induce the two-magnon scattering, observing the four-fold symmetry of in-plane ΔH anisotropy. They controlled the insertion of the misfit dislocation networks by changing the structure and thickness of cap layers and correlated them to the two-magnon scattering observed. This demonstration suggests that the choice of the layer structure/materials is critically dependent on the number/type of defects in epitaxial thin film stacks. In our case with 1.0(7ML) nm Fe sandwiched by GaAs, we interestingly observed a uniaxial anisotropy in the in-plane ΔH shown to be from two-magnon scattering effect. This, together with the two-magnon phenomenology, suggests that defects in our Fe layer causes more (less) spin-wave scattering along the strong-(weak-)relaxation direction, i.e., [$\bar{1}$10] ([110]). We can, therefore, speculate as to the presence of defects elongated along [110] in our Fe layer. Moosbuhler *et al.*[32] used scanning tunnel microscopy to observe the initial growth of Fe on GaAs and confirmed that the initial growth of Fe on GaAs is three-dimensional, forming row structures both along [$\bar{1}$10] and [110], depending on the type of GaAs reconstructed surfaces. Since the thickness of our Fe layer is 1 nm, it can be plausible that the morphology of the Fe layer descends from the initial growth characteristic, acting as a source of the two-magnon scattering. However, we must note that the size of the morphological defects or roughness should be much larger than atomic-scale defects. We also add that the observed two-fold symmetry in the two-magnon scattering when reducing the film thickness is the same trend as observed in the magnetic anisotropy of ultra-thin Fe on GaAs.[36]

In conclusion, we have studied magnetic relaxation of ultra-thin epitaxial Fe layer grown on GaAs and found that

TABLE I. Magnetic anisotropy and relaxation parameters of the Fe microbars

	Bar direction	$\mu_0 M_{eff}$ (T)	$\mu_0 H_2$ (T)	γ (rad GHz/T)	$\mu_0 \Delta H_{inh}$ (10^{-3} T)	α (10^{-3})	$\sum_i \Gamma_i f_i(135°)$ (GHz)	$\sum_i \Gamma_i f_i(45°)$ (GHz)	$\Delta\theta$ (deg)
Sample 1	010	0.545	0.108	187	3.3	7.6	4.7	0.2	0.8
Sample 2	100	0.780	0.110	188	3.5	7.3	5.2	0.2	0.5

there is an in-plane uniaxial anisotropy of magnetic relaxation. By making full use of other parameters obtained from FMR measurements, we calculated the symmetry of the in-plane ΔH components and determined that only the two-magnon scattering mechanism can explain the uniaxial anisotropy. Out-of-plane angle and frequency dependence of the linewidth further support the conclusion of two-magnon scattering occurring in the 1 nm Fe. The reported results are additional evidence that defect-induced magnon processes become increasingly important for nanoscale ferromagnets and understanding/control of these effects will be extremely crucial for future nanoscale spintronic devices.

The authors acknowledge Dr. Kh. Zakeri and Dr. G. Woltersdorf for their helpful discussions. H.K. acknowledges JSPS, JST, and EPSRC for their financial supports. K.O. acknowledges EU Grant No. FP7-215368 SemiSpinNet. A.J.F. acknowledges the support of a Hitachi research fellowship. The authors are grateful for the support from EU Grant No. FP7-214499 NAMASTE.

[1]I. Zutic, J. Fabian, and S. D. Sarma, Rev. Mod. Phys. **76**, 323 (2004).
[2]J. C. Slonczewski, J. Magn. Magn. Mater. **159**, L1 (1996); L. Berger, Phys. Rev. B **54**, 9353(1996).
[3]D. C. Ralph and M. D. Stiles, J. Magn. Magn. Mater. **320**, 1190 (2008).
[4]V. V. Kruglyak, S. O. Demokritov, and D. Grundler, J. Phys. D: Appl. Phys. **43**, 264001 (2010).
[5]A. A. Serga, A. V. Chumak, and B. Hillebrands, J. Phys. D: Appl. Phys. **43**, 264002 (2010).
[6]Y. Tserkovnyak, A. Brataas, and G. E. W. Bauer, Phys. Rev. Lett. **88**, 117601 (2002).
[7]B. Heinrich, Y. Tserkovnyak, G. Woltersdorf, A. Brataas, R. Urban, and G. E. W. Bauer, Phys. Rev. Lett. **90**, 187601 (2003).
[8]S. Mizukami, Y. Ando, and T. Miyazaki, Phys. Rev. B **66**, 104413 (2002).
[9]E. Saitoh, M. Ueda, H. Miyajima, and G. Tatara, Appl. Phys. Lett. **88**, 182509 (2006).
[10]K. Ando, S. Takahashi, J. Ieda, H. Kurebayashi, T. Trypiniotis, C. H. W. Barnes, S. Maekawa, and E. Saitoh, Nature Mater. **10**, 655 (2011).
[11]A. G. Gurevich and G. A. Melkov, *Magnetization Oscillations and Waves* (CRC, Boca Raton, FL, 1996).
[12]T. L. Gilbert, IEEE Trans. Magn. **40**, 3443 (2004).
[13]H. Kurebayashi, O. Dzyapko, V. E. Demidov, D. Fang, A. J. Ferguson, and S. O. Demokritov, Nature Mater. **10**, 660 (2011).
[14]M. Sparks, R. Loudon, and C. Kittel, Phys. Rev. **122**, 791 (1961).
[15]M. Hurben and C. E. Patton, J. Appl. Phys. **83**, 4344 (1998).
[16]R. Arias and D. L. Mills, Phys. Rev. B **60**, 7395 (1999).
[17]R. D. McMichael, M. D. Stiles, P. J. Chen, and W. F. Egelhoff, Jr., J. Appl. Phys. **83**, 7037 (1998).
[18]R. Urban, B. Heinrich, G. Woltersdorf, K. Ajdari, K. Myrtle, J. F. Cochran, and E. Rozenberg, Phys. Rev. B **65**, 020402 R (2001).
[19]R. D. McMichael, D. J. Twisselmann, and A. Kunz, Phys. Rev. Lett. **90**, 227601 (2003).
[20]G. Woltersdorf and B. Heinrich, Phys. Rev. B **69**, 184417 (2004).
[21]G. Woltersdorf, M. Buess, B. Heinrich, and C. H. Back, Phys. Rev. Lett. **95**, 037401 (2005).
[22]J. Lindner, I. Barsukov, C. Raeder, C. Hassel, O. Posth, R. Meckenstock, P. Landeros, and D. L. Mills, Phys. Rev. B **80**, 224421 (2009).
[23]K. Lenz, H. Wende, W. Kuch, K. Baberschke, K. Nagy, and A. Janossy, Phys. Rev. B **73**, 144424 (2006).
[24]Kh. Zakeri, J. Lindner, I. Barsukov, R. Meckenstock, M. Farle, U. von Hörsten, H. Wende, W. Keune, J. Rocker, S. S. Kalarickal, K. Lenz, W. Kuch, K. Baberschke, and Z. Frait, Phys. Rev. B **76**, 104416 (2007).
[25]J. Dubowik, K. Zaleski, H. Glowinski, and I. Goscianska, Phys. Rev. B **84**, 184438 (2011).
[26]I. Barsukov, P. Landeros, R. Meckenstock, J. Lindner, D. Spoddig, Z.-A Li, B. Krumme, H. Wende, D. L. Mills, and M. Farle, Phys. Rev. B **85**, 014420 (2012).
[27]A. A. Tulapurkar, Y. Suzuki, A. Fukushima, H. Kubota, H. Maehara, K. Tsunekawa, D. D. Djayaprawira, N. Watanabe, and S. Yuasa, Nature **438**, 339 (2005).
[28]N. Mecking, Y. S. Gui, and C. M. Hu, Phys. Rev. B **76**, 224430 (2007).
[29]A. Yamaguchi, K. Motoi, A. Hirohata, H. Miyajima, Y. Miyashita, and Y. Sanada, Phys. Rev. B **78**, 104401 (2008).
[30]D. Fang, H. Kurebayashi, J. Wunderlich, K. Vborn, L. P. Zrbo, R. P. Campion, A. Casiraghi, B. L. Gallagher, T. Jungwirth, and A. J. Ferguson, Nat. Nanotechnol. **6**, 413 (2011).
[31]M. Farle, Rep. Prog. Phys. **61**, 755 (1998).
[32]R. Moosbuhler, F. Bensch, M. Dumm, and G. Bayreuther, J. Appl. Phys. **91**, 8757 (2002).
[33]S. V. Vonsovski, *Ferromagnetic Resonance* (Pergamon, Oxford, 1960).
[34]P. Landeros, R. E. Arias, and D. L. Mills, Phys. Rev. B **77**, 214405 (2008).
[35]M. Hurben, D. R. Franklin, and C. E. Patton, J. Appl. Phys. **81**, 7458 (1997).
[36]G. Wastlbauer and J. A. C. Bland, Adv. Phys. **54**, 137 (2005).